

MTLoc: A Confidence-Based Source-Free Domain Adaptation Approach For Indoor Localization

Negar Mehregan, Berk Bozkurt, Eric Granger, Mohammadjavad Hajikhani, Mohammadhadi Shateri

Abstract—Various deep learning models have been developed for indoor localization based on radio-frequency identification (RFID) tags. However, they often require adaptation to ensure accurate tracking in new target operational domains. To address this challenge, unsupervised domain adaptation (UDA) methods have been proposed to align pre-trained models with data from target environments. However, they rely on large annotated datasets from the initial domain (source). Source data access is limited by privacy, storage, computational, and transfer constraints. Although many source-free domain adaptation (SFDA) methods address these constraints in classification, but applying them to regression models for localization remains challenging. Indeed, target datasets for indoor localization are typically small (few features and samples) and noisy, and adapting regression models requires high-confidence target pseudo-annotation to avoid over-training. In this paper, a specialized mean-teacher method called MTLoc is proposed for SFDA. MTLoc updates the student network using noisy data and teacher-generated pseudo-labels. The teacher network maintains stability through exponential moving averages. To further ensure robustness, the teacher’s pseudo-labels are refined using k -nearest neighbor correction. MTLoc allows for self-supervised learning on target data, facilitating effective adaptation to dynamic and noisy indoor environments. Validated using real-world data from our experimental setup with INLAN Inc., our results¹ show that MTLoc achieves high localization accuracy under challenging conditions, significantly reducing localization error compared to baselines, including the state-of-the-art adversarial UDA approach with access to source data.

Index Terms—Deep learning, unsupervised domain adaptation, source-free domain adaptation, mean-teacher models, indoor localization.

I. INTRODUCTION

ROBUST and reliable localization systems aim to revolutionize positioning in fields like the Internet of Things [1], and Augmented Reality [2]. Various indoor localization techniques are being studied, in which WiFi-based methods are attracting the most attention due to their compatibility, cost-effectiveness, and wide applicability [3]–[5].

As GPS signals are proven to be ineffective for localization due to signal deflection and multipath-related issues [6], different technologies are introduced, with qualifications varying based on the type of tag applied. Among others, ultrawideband (UWB) tags [7], [8] with high-precision accuracy

N. Mehregan, E. Granger, and M. Shateri are with the LIVIA, Department of Systems Engineering, ETS Montreal, Canada (e-mails: negar.mehregan.1@ens.etsmtl.ca, eric.granger@etsmtl.ca, mohammadhadi.shateri@etsmtl.ca).

B. Bozkurt and M. Hajikhani are with INLAN Inc., Montreal, Canada (e-mails: b.bozkurt@inlantech.com, m.hajikhani@inlantech.com).

¹Code and datasets: <https://github.com/negarmehregan/Indoor-Localization/tree/main>

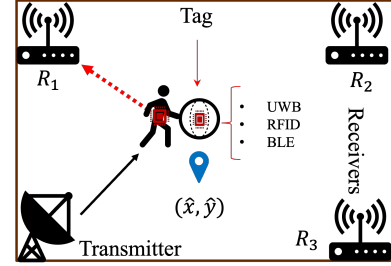


Fig. 1: Illustration of an indoor localization system for tracking objects and individuals in real-time having three receivers and a transmitter by employing tags such as UWB, RFID, BLE.

and low power usage, radio frequency identification (RFID) tags [9], [10] with lower cost and long-range communication, and Bluetooth low energy (BLE) tags [11], [12], a medium range, energy-efficient technology, are utilized in localization models. Tag-based tracking models are employed to monitor key assets’ location, ensure safety, and localize objects for healthcare applications [13]–[15]. Fig. 1 illustrates the application of an indoor localization system, in which a signal is passed from the transmitter to the receiver, after reaching the tagged object. A typical indoor positioning system incorporates receivers, transmitters, and tags for data collection. In various studies, through using receivers, different types of data were acquired from tags including received signal strength [16]–[18], Phase, Channel Impulse Response [19], [20], channel state information (CSI) [21], [22], angle of arrival [23]–[25], and radio frequency [26], [27]. However, the inaccuracies caused by signal attenuation, and distortion, remain a challenge, particularly in complex environments in which multipath components and non-line-of-sight effects stand out as the most concerning [20], [28]. To address these issues, various deep learning-based techniques are proposed for indoor localization.

Several AI-based techniques are being developed to address indoor localization problems. For instance, with MF-FALoc [21] CSI fingerprints are fed into a convolutional neural network (CNN), tackling multipath and non-line-of-sight effects. Furthermore, Rao et al. [21] remove environmental noise by utilizing waveform diversity and detection, and implement a feature fusion system to merge the multi-antenna feature matrices, resulting in fine-grained fingerprints. Some studies, such as Chen et al. [29], apply 1D-CNN for RF-based environment classification, while others, like Yan et al. [30], use 2D deep CNNs for CSI feature extraction to improve

localization accuracy. Se-Loc [31], is another CNN-driven approach with a security-enhanced semi-supervised indoor localization technique by integrating a denoising autoencoder (AE), aiding in improving fingerprinting localization. This model has a Pearson correlation coefficient-based access point selection system to eliminate the contaminated access points. Certain research initiatives, such as in [32], use AE for spatial feature extraction. Likewise, in [33] and [28], a variational AE is being applied to extract key position-related features and reduce environmental noise to solve localization and multipath challenges. Some researchers merge recurrent neural networks with AE such as [34], where a stacked AE, extracting key features, is combined with an attention-based long short-term memory network, enhancing its localization accuracy. On the other hand, Liu et al. [35] uses gated recurrent units for feature extraction, while Chen et al. [36] apply a deep LSTM with a local feature extractor to process RSSI fingerprints, capturing temporal dependencies through a regression layer for localization. Some use generative models for data augmentation [37]–[39], improving localization accuracy.

Previous studies discover the impact of environmental change on the data [40], [41]. As mentioned by [42], CSI data is affected by any changes in the environment, hence, a localization system might not perform well in a new environment. Therefore, they propose an unsupervised domain adaptation (UDA) method in which the source domain’s model is fine-tuned to be applicable in a new distinct but associated domain, where the ground truth data is not accessible. Given a pre-trained model utilizing labeled source data collected from Warehouse A, the objective is to evaluate its performance in a different environment, Warehouse B. The primary challenge lies in the fact that the new domain (Warehouse B) may produce substantially different object-related signals, possibly due to variations in the positions of transmitters and receivers. However, retraining the model is infeasible due to the lack of annotated data from Warehouse B. This scenario falls under the framework for UDA.

Currently, UDA approaches can be classified into three main categories [43]: a) domain distribution alignment [44]–[46] b) adversarial learning to extract domain-invariant representation [47]–[49], and c) model fine-tuning through self-supervision [50]–[52]. In the context of indoor localization, most UDA approaches rely on adversarial learning through the use of the gradient reversal layer (GRL), as Zhang et al. [53] utilizing a semi-supervised graph convolutional network based model with received signal strength indicator data, Xu et al. [54] with a Gaussian noise infused co-teaching mechanism, Zhang et al. [55] in which dynamic adversarial adaptation networks is applied to eliminate any inconsistency in both global and local discriminators, and Prasad et al. [56], applying an AE for dimension reduction purposes as well as gradient reversal layer to create a domain invariant features. Additionally, discrepancy-based models, aligning source and target domain distributions are created, as shown in [57], in which the Grassmann manifold is employed for dimensional reduction purposes while preserving the integrity of original data, and maximum mean discrepancy to ensure localization accuracy. Certain studies conducted hybrid mechanisms by using both

generative and GRL-based approaches in their models, for instance, [58] and [42] in which generative models are used for data augmentation, using variational AE and adversarial AE respectively. In [58], the researcher applied a domain-adaptive classifier incorporating a feature extractor as well as a classification-reconstruction layer. Meanwhile, in [42], a CNN model serves as a feature extractor, with a gradient reversal layer-based discriminator and location predictor networks.

Nevertheless, as there are concerns regarding the data-privacy issues in UDA, especially, in case of having sensitive information in the source domain, as mentioned by [59], therefore, to avoid data leakage, source-free based models could be applied for localization purposes, aiding in achieving high accuracy across different domains while respecting the privacy concerns. On top of that, source-free (unsupervised) domain adaptation (SFDA) systems reduce computable costs and facilitate data storage, and transfer [60], [61]. Moreover, in certain cases, regulations prevent any data transfer, while some companies also aim to maintain the ownership of their data, thus, making source-free models more practical [61]. Furthermore, the scalability of SFDA models enables organizations to adapt accordingly to different target environments [61], [62]. SFDA is considered a way to create an efficient domain-invariant system as discussed by Fang et al. [60] who conducted research in this area, providing a detailed survey regarding image-based studies.

To the best of our knowledge, no method for SFDA has been proposed for indoor localization. Of the current SFDA methods, the mean teacher framework is particularly well-suited for regression-based indoor localization. In practice, target datasets for indoor localization are often limited and noisy, making domain adaptation reliant on highly confident pseudo-labels. Researchers such as Yeonguk et al. [63] have used this technique due to its EMA-based stabilization, which produces stable pseudo labels through consistency regularization. Although it is a simple approach, it ensures efficient performance in source-free scenarios while leveraging self-supervision. Motivated by these characteristics, we introduce mean teacher localization (MTLoc) for SFDA, a self-supervised method leveraging a mean teacher framework. This approach uses a teacher-student architecture, where both networks are initialized with a localizer, pre-trained on source data. The student model is fine-tuned on noisy target domain data using pseudo labels generated by the teacher network, enabling effective adaptation without access to source data. To further improve performance, we propose an enhanced model, MTLoc with confidence, where the teacher’s uncertain pseudo-labels are corrected using k -nearest neighbors (k -NN), and the student model is trained exclusively on the most confident ones generated by the teacher network. This refinement improves the reliability of the adaptation by focusing on high-certainty predictions, reducing variations, thereby enhancing the robustness of the SFDA process.

The main contributions of this paper are as follows.

- We present the MTLoc, an SFDA method for indoor localization, by leveraging a self-supervised knowledge distillation framework to adapt from small and noisy target data.

- An improved confidence-based variant of MTLoc is proposed, where uncertain pseudo labels generated by the teacher network are refined using a k -NN strategy to compute a weighted average of the k most confident pseudo labels. This ensures that the student network is trained exclusively on high-confidence labels, enhancing overall model robustness.
- We conducted a comprehensive data collection process to develop three datasets—Ceiling (source), Cross, and Square (targets)—at the INLAN Inc. testing facility. This setup involved four receivers, a transmitter equipped with dipole antennas, and an RFID tag, providing a robust evaluation environment for the proposed method. MTLoc is validated on this real-world data and significantly outperforms the state-of-the-art adversarial UDA model.

This paper is organized as follows. Section II provides a problem definition for SFDA, followed up by details on our domain adaptation baseline method. In section III, we provide specifics on our proposed confidence-based SFDA method. Section IV presents our methodology for experimental validation (i.e., data collection, protocol, performance measures), as well as our analysis of experimental results.

Notation and Conventions: We denote random variables using uppercase letters (e.g., X, Y) and their specific realizations using lowercase letters (e.g., x, y). The notation $p(x)$ refers to the probability distribution of the random variable X , while $p(x|y)$ represents the conditional distribution of X given Y . The expectation of a function with respect to the joint distribution of all random variables is denoted by $\mathbb{E}[\cdot]$.

II. PROBLEM DEFINITION AND BASELINE OVERVIEW

A. Problem Formulation:

Consider an indoor localization framework consisting of N receivers and a single transmitter. The transmitter emits signals that interact with objects within the environment, and these signals are subsequently captured by the receivers. The objective is to develop an object localization system by analyzing the signals recorded by the receivers. Let Z denote the random variable representing the signals recorded by the receivers, and let (X, Y) represent the joint random variables corresponding to the true location associated with the recorded signal Z . The goal is to learn an object localizer defined as the mapping $\mathcal{M}(\cdot; \theta) : \mathcal{Z} \rightarrow \mathcal{X} \times \mathcal{Y}$ parameterized by θ , which produces an approximation (\hat{X}, \hat{Y}) of the true location for each observed signal Z , i.e. $(\hat{X}, \hat{Y}) = (Z; \theta)$. To optimize the parameters θ of the localizer, we employ Bayesian optimization by maximizing the log-likelihood of the true location given the estimated location as follows:

$$\theta^* = \arg \max_{\theta} \log p_{X,Y|\hat{X},\hat{Y}}(x, y | \hat{x}, \hat{y}), \quad (1)$$

where depending on the assumed statistical model of the localization errors, this maximum likelihood estimation leads to different loss functions.

Gaussian Error Model [64]: Assuming the localization errors $(X - \hat{X}, Y - \hat{Y})$ follow a bivariate Gaussian distribution

with zero mean and covariance matrix Σ , the negative log-likelihood function becomes:

$$-\log p(x, y | \hat{x}, \hat{y}) \propto \begin{pmatrix} x - \hat{x} \\ y - \hat{y} \end{pmatrix}^{\top} \Sigma^{-1} \begin{pmatrix} x - \hat{x} \\ y - \hat{y} \end{pmatrix} \quad (2)$$

If Σ is proportional to the identity matrix, the expression simplifies, and maximizing the likelihood presented in Equ. (1) is equivalent to the following problem:

$$\theta^* = \arg \min_{\theta} \mathbb{E}_{p_{X,Y,Z}} \left[(X - \hat{X})^2 + (Y - \hat{Y})^2 \right], \quad (3)$$

where the expectation is taken over the joint distribution of $p_{X,Y,Z}$.

Laplacian Error Model [64]: Alternatively, considering the localization errors follow a bivariate Laplacian distribution and assuming independence between error in X and Y , the joint probability density function can be written as follows:

$$p(x, y | \hat{x}, \hat{y}) = \left(\frac{1}{\sqrt{2}b} \right)^2 \exp \left(-\frac{|x - \hat{x}| + |y - \hat{y}|}{\sqrt{2}b} \right) \quad (4)$$

where $b > 0$ is the scale parameter. In this case, the negative log-likelihood function is simplified to:

$$-\log p(x, y | \hat{x}, \hat{y}) = \frac{1}{\sqrt{2}b} (|x - \hat{x}| + |y - \hat{y}|) + 2 \log(\sqrt{2}b) \quad (5)$$

Ignoring the constant terms, maximizing the likelihood in Equ. (1) corresponds to the following problem:

$$\theta^* = \arg \min_{\theta} \mathbb{E}_{p_{X,Y,Z}} \left[|X - \hat{X}| + |Y - \hat{Y}| \right] \quad (6)$$

In this work, either formulation (3) or (6) could be used for optimizing the parameters θ of localizer $\mathcal{M}(\cdot; \theta)$, however, we applied equation (6). After training $\mathcal{M}(\cdot; \theta)$ using data from a source domain \mathbf{D}_s characterized by the joint distribution $p_{X,Y,Z}^s$, we aim to adapt it to a new target (operational) domain \mathbf{D}_t , where the joint distribution is $p_{X,Y,Z}^t \neq p_{X,Y,Z}^s$. The discrepancy between the source and target domains poses a challenge, as the localizer trained on \mathbf{D}_s may perform poorly on \mathbf{D}_t due to distribution shifts. Our objective is to adapt $\mathcal{M}(\cdot; \theta)$ to perform well in the target domain using an unlabeled \mathbf{D}_t .

B. Baselines:

In this study, we considered several baselines including a source-only pre-adaptation model and an oracle approach trained on labeled target datasets [65], [66]. Among UDA approaches created for indoor localization, adversarial UDA and discrepancy-based models are prominent, with the state-of-the-art focusing predominately on the use of GRL-based adversarial UDA techniques. Thereby, we evaluated an adversarial UDA method that leverages a GRL-based model. This approach is inspired by FreeLoc [42], an adaptation of Domain-Adversarial Neural Network (DANN) [67], which facilitates domain alignment through adversarial training, and serves as another baseline. As illustrated in Fig. 2, the framework assumes access to a labeled source dataset, $\mathbf{D}_s = \{z_s^{(i)}, (x_s^{(i)}, y_s^{(i)})\}_{i=1}^{N_s}$ with distribution $p_{X,Y,Z}^s$, and an unlabeled target dataset, $\mathbf{D}_t = \{z_t^{(j)}\}_{j=1}^{N_t}$ with distribution p_{Z}^t .

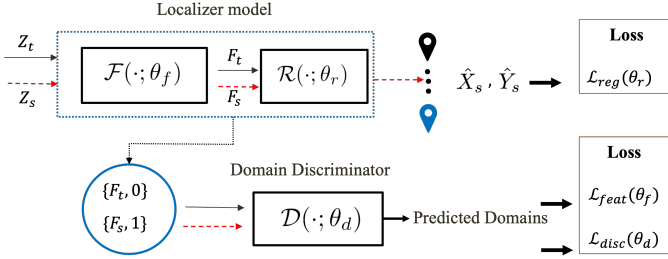


Fig. 2: *System overview*: The source data Z_s and the unlabeled target data Z_t are processed through our Localizer model, which comprises a feature extractor $\mathcal{F}(\cdot; \theta_f)$ and a regressor $\mathcal{R}(\cdot; \theta_r)$. The source data Z_s is used to generate predictions, while the feature extractor $\mathcal{F}(\cdot; \theta_f)$ is trained to deceive the discriminator $\mathcal{D}(\cdot; \theta_d)$.

Here, z represents the signals received by the receivers, while (x, y) denotes the object location in the corresponding domain.

This framework leverages a localizer model that comprises two core components: a feature extractor $\mathcal{F}(\cdot; \theta_f)$, which maps input signals to a latent feature space, and a regressor $\mathcal{R}(\cdot; \theta_r)$, which predicts the object's location based on the extracted features. Additionally, a domain discriminator $\mathcal{D}(\cdot; \theta_d)$ is incorporated to facilitate domain adaptation. During the adaptation process, the feature extractor processes received signals from both the source and target domains, while the domain discriminator is trained to distinguish between features from these domains. Concurrently, the regressor is optimized using labeled source data to predict object locations accurately. The feature extractor, however, is adversarially trained to both confuse the domain discriminator and preserve localization accuracy for the regressor.

The training objective is formalized such that the feature extractor aims to align the source and target domains in the feature space. This alignment occurs when the domain discriminator can no longer differentiate between the two domains, thus enabling the regressor trained on source data to generalize effectively to the target domain.

$$\min_{\theta_f, \theta_r} \max_{\theta_d} \mathbb{E} [\log \mathcal{D}(\mathcal{F}(Z_s))] + \mathbb{E} [\log(1 - \mathcal{D}(\mathcal{F}(Z_t)))] + \mathbb{E} [|X_s - \hat{X}_s| + |Y_s - \hat{Y}_s|] \quad (7)$$

The first two terms represent the adversarial objective, where the feature extractor \mathcal{F} seeks to mislead the domain discriminator \mathcal{D} . The final term represents the regression loss, encouraging the regressor \mathcal{R} to minimize the distance between the predicted and true object locations for the source domain. Through this adversarial training, feature alignment between the source and target domains is achieved, enabling robust location prediction in the target domain. It should be mentioned that for training each model, the following loss functions are defined based on Equ. (7) where the expectations are approximated empirically. More precisely, let $\{z_s^{(b)}, (x_s^{(b)}, y_s^{(b)})\}_{b=1}^B$ and $\{z_t^{(b)}\}_{b=1}^B$ be a set of B data samples from source and target respectively. The loss functions for training each

network in Fig. 2 are presented in equations (8)(9)(10).

$$\mathcal{L}_{\text{reg}}(\theta_r) = \mathbb{E}_{p_{\hat{X}_s, Y_s, Z}} [|X_s - \hat{X}_s| + |Y_s - \hat{Y}_s|] \approx \frac{1}{B} \sum_{b=1}^B [|x_s^{(b)} - \hat{x}_s^{(b)}| + |y_s^{(b)} - \hat{y}_s^{(b)}|] \quad (8)$$

$$\mathcal{L}_{\text{disc}}(\theta_d) = -\mathbb{E}_{p_{Z_s}} [\log \mathcal{D}(\mathcal{F}(Z_s))] - \mathbb{E}_{p_{Z_t}} [\log(1 - \mathcal{D}(\mathcal{F}(Z_t)))] \approx \frac{-1}{B} \sum_{b=1}^B [\log \mathcal{D}(\mathcal{F}(z_s^{(b)})) + \log(1 - \mathcal{D}(\mathcal{F}(z_t^{(b)})))] \quad (9)$$

$$\mathcal{L}_{\text{feat}}(\theta_f) = \mathcal{L}_{\text{reg}} - \mathcal{L}_{\text{disc}} \quad (10)$$

The detailed training procedure of the feature extractor, regressor, and discriminator for our baseline model adversarial UDA is given in Algorithm 1 which illustrates how these networks are updated depending on their functionality. In the next section, our proposed method for indoor localization will be discussed. Unlike state-of-the-art approaches, our UDA method is source-free, meaning that it does not rely on access to source data \mathbf{D}_s for adaptation.

Algorithm 1: Domain Adaptation with Access to Source Data

- 1: **Input:** Labeled Source data Z_s , Target data Z_t
 - 2: **Initialize:** Feature Extractor $\mathcal{F}(\cdot; \theta_f)$, Regressor $\mathcal{R}(\cdot; \theta_r)$, and Discriminator $\mathcal{D}(\cdot; \theta_d)$
 - 3: **while** not converged **do**
 - 4: Extract features: $F_s = \mathcal{F}(Z_s; \theta_f)$, $F_t = \mathcal{F}(Z_t; \theta_f)$
 - 5: Update θ_r by $\nabla_{\theta_r} \mathcal{L}_{\text{reg}}$ (Equ. (8))
 - 6: Train Discriminator $\mathcal{D}(\cdot; \theta_d)$ on (F_s, F_t)
 - 7: Update θ_f by $\nabla_{\theta_f} \mathcal{L}_{\text{feat}}$ (Equ. (10)) Received Signal Strength Indicator data
 - 8: Update θ_d by $\nabla_{\theta_d} \mathcal{L}_{\text{disc}}$ (equation (9))
 - 9: **end while**
-

III. THE PROPOSED MTLOC METHOD

In this study, an SFDA approach is proposed for indoor localization, called mean teacher localization (MTLoc), illustrated in Fig. 3. As the current approaches are conditioned on the availability of the source domain data, making them not feasible in real-world scenarios [60], we developed a source-free model. In this technique, two models are trained to ensure the quality and effectiveness of the training. This approach implements two networks: 1) teacher network $\mathcal{T}(\cdot; \theta_t)$ [60] 2) student network $\mathcal{S}(\cdot; \theta_s)$ [60] where the Teacher model is developed to have similar insights to the Students', aiding in efficient generalization to new data. In the first stage, the Teacher and student networks are initialized using a pre-trained source localizer, $\mathcal{M}(\cdot; \theta)$ with a regression loss, minimizing the average absolute differences from the predicted and ground-truth parameters is shown in the Equ. (8).

In this approach, the teacher network receives the unlabeled target data Z_t , while the student network receives an augmented version by using an additive Gaussian noise $\mathcal{N}(0, \sigma^2)$ with a pre-determined variance σ^2 [68]. teacher network $\mathcal{T}(\cdot; \theta_t)$ generates pseudo labels, (X'_t, Y'_t) , for each

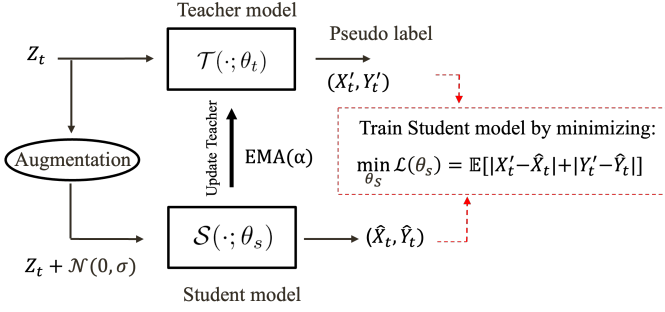


Fig. 3: *MTLoc*: The unlabeled target data (Z_t) is passed to the Teacher model $\mathcal{T}(\cdot; \theta_t)$ to generate pseudo labels (X'_t, Y'_t) , while undergoing an augmentation process, through Gaussian Noise, allowing the Student model $\mathcal{S}(\cdot; \theta_s)$ to proceed with the prediction \hat{X}_t, \hat{Y}_t while minimizing the Knowledge Distillation Loss L_{KD} .

sample received from Z_t . These newly derived pseudo labels are considered as the ground truth for Student model $\mathcal{S}(\cdot; \theta_s)$ which would be used while proceeding with predictions, (\hat{X}_t, \hat{Y}_t) . During the training process, the teacher network's parameters are updated by applying an Exponential Moving Average (EMA) process based on the Students', with a pre-determined decay rate α . As the student network is trained to imitate the Teacher's performance and replicate its generated pseudo labels, by applying the loss function (11), any data degradation would be minimized, resulting in a stable and aligned network.

$$\begin{aligned} \mathcal{L}(\theta_s) &= \mathbb{E} \left[|X'_t - \hat{X}_t| + |Y'_t - \hat{Y}_t| \right] \\ &\approx \frac{1}{B} \sum_{b=1}^B \left[|x_t^{(b)} - \hat{x}_t^{(b)}| + |y_t^{(b)} - \hat{y}_t^{(b)}| \right] \end{aligned} \quad (11)$$

Algorithm 2: Confidence-based source-free UDA with self-supervised knowledge distillation

- 1: **Given:** A localizer with parameters $\mathcal{M}(\cdot; \theta)$, (unlabeled) target data z_t , and decay rate α
 - 2: Initialize parameters of Teacher $\mathcal{T}(\cdot; \theta_t)$ & Student $\mathcal{S}(\cdot; \theta_s)$ with $\mathcal{M}(\cdot; \theta)$
 - 3: **for** number of adaptation steps **do**
 - 4: Determine confident scores, correct labels (Algorithm 3)
 - 5: Get a batch of target data $\{z_t^{(b)}\}_{b=1}^B$ with associated Pseudo Labels $\{(x'_t, y'_t)^{(b)}\}_{b=1}^B$.
 - 6: Do data augmentation at the Student's input $\{z_t^{(b)} + \epsilon^{(b)}\}$ where $\epsilon^{(b)} \sim \mathcal{N}(0, \sigma)$
 - 7: Update Student by $\nabla_{\theta_s} [\mathcal{L}(\theta_s)]$ (see equation 11)
 - 8: Update Teacher using EMA: $\theta_t \leftarrow \alpha \cdot \theta_s + (1 - \alpha) \cdot \theta_t$
 - 9: **end for**
-

To enhance the performance of our *MTLoc* model, we developed an enhanced approach, built on a confidence-based methodology, illustrated as Fig. 4, called *MTLoc with confidence*, in which every unconfident sample z_t and its generated pseudo labels undergo a correctional process, modifying the uncertain predictions. This aids the Student model in being trained on more confident labels. In our correction module, $\mathcal{T}(\cdot; \theta_t)$ generates pseudo labels (x'_t, y'_t) using a noisy version of the unlabeled target data z_t . By repeating this process, the standard deviation σ of the measurements is determined.

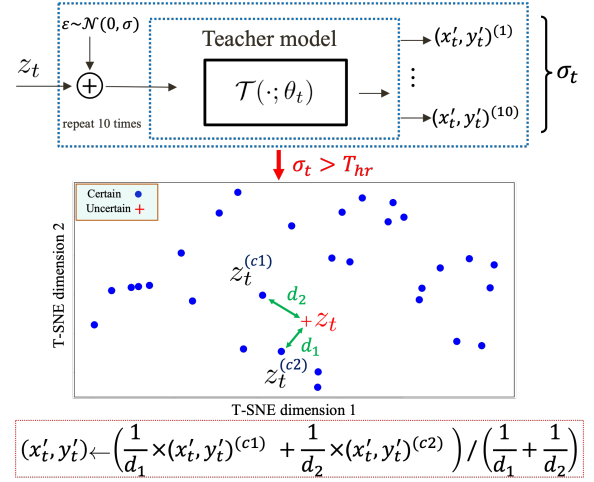


Fig. 4: *MTLoc with confidence*: z_t together with the generated pseudo labels (x'_t, y'_t) go through a correction process in which the uncertain labels would be identified based on a threshold (T_{hr}) and modified using k -NN (with $k = 2$). The t -SNE plot shown above highlights an uncertain sample z_t being corrected using two nearest certain ones. The newly modified pseudo label (x'_t, y'_t) is considered as ground truth for our Student model to generate predictions and update the Teacher model with EMA while applying distillation loss.

Each sample is tested 10 times, and these repeated trials provide the basis for calculating the standard deviations for both x and y . These uncertain variables would be corrected by employing a k NN-based technique, if the standard deviation of generated labels is higher than an assigned Threshold (T_{hr}). For additional details regarding the implementation of the threshold, please refer to Appendix C. In this mechanism, an uncertain pseudo label (x'_t, y'_t) would be modified by performing a weighted average of the k confident neighboring labels as illustrated below:

$$(x'_t, y'_t) \leftarrow \frac{\sum_{i=1}^K \frac{1}{d_i} \times (x'_t, y'_t)^{(c_i)}}{\sum_{i=1}^K \frac{1}{d_i}} \quad (12)$$

with d_i being the Euclidean Distance between the uncertain and the i -th closest confident samples while the $(x'_t, y'_t)^{(c_i)}$ is the associated confident pseudo label.

Algorithm 3: Confidence scores and label generation process for SFDA approach

- 1: **Input:** Unlabeled target data z_t , Teacher Model $\mathcal{T}(\cdot; \theta_t)$
 - 2: Compute (x'_t, y'_t) for 10 runs with additive noise $\mathcal{N}(0, \sigma)$
 - 3: Identify uncertain pseudo labels as those with $\sigma_t > T_{hr}$, where σ_t is the standard deviation of the 10 runs and T_{hr} is a pre-determined threshold.
 - 4: **for** each uncertain sample z_t **do**
 - 5: Correct the Pseudo Label (x'_t, y'_t) by using the weighted average of confident labels with k -nearest neighbors (see equation 12)
 - 6: **end for**
-

The training along with the specifics of the pseudo label correctional process of our introduced confidence-based *MTLoc* model is detailed in Algorithms 2 and 3.

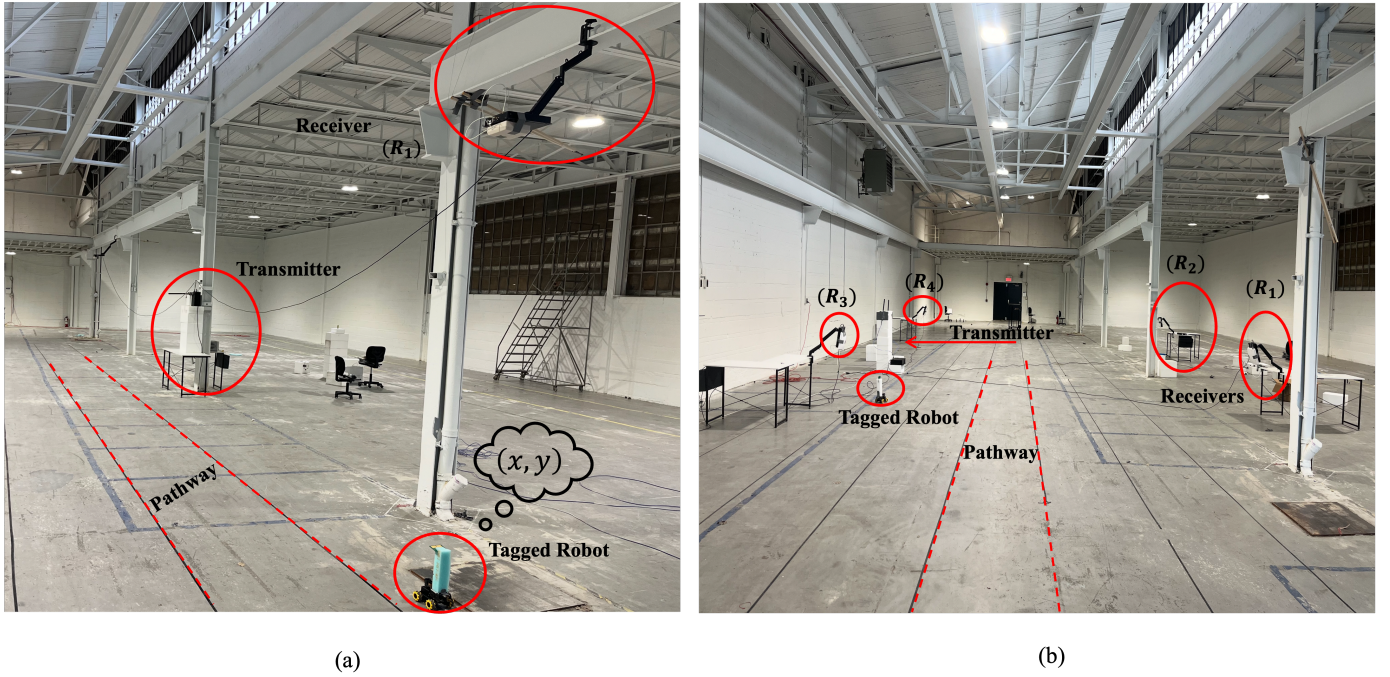


Fig. 5: Experimental setup of INLAN's Ceiling and Square datasets where (a) is the source domain formation with receivers positioned on the ceiling, and a transmitter activating RFID tag, located in the robot moving on pre-determined pathways and (b) the target domain's setup with receivers installed in the square position.

IV. RESULTS AND DISCUSSION

A. Experimental Setup

1) Environment and devices

The experiments were performed in INLAN's testing facility [69] where a transmitter and four receivers are deployed in different configurations that are specified in the datasets provided (see Fig. 5). The transmitter is equipped with a dipole stick antenna (2 stick antennas for cross and square datasets) with 2.15 dBi gain, and each receiver is equipped with a patch antenna with 16 dBi gain. Note that for the locations of the devices, the bottom left corner of the warehouse is considered as the origin, all units are in terms of meters and the positions are given in the form (x, y) where x and y denotes the horizontal and vertical axes, respectively. Configuration details are as follows:

- Ceiling configuration: Transmitter is located at (8.5, 13) meter, receivers are located at the points (8.5, 5), (0.5, 13.6), (8.5, 21.9), (17.5, 14). The transmitter antenna is placed parallel to the ground at a height of 1.8 m. Receivers are mounted on the ceiling at a height of 3 m with each patch antenna parallel to the ground. The tag is also parallel to the ground and elevated at a height of 0.36 m.
- Square configuration: Transmitter is located at (5, 9) meter, receivers are located at the points (0, 1.5), (0, 15), (11, 14), (11, 2.5). Transmitter antennae separated by 0.4 m are placed perpendicular to the ground at a height of 1.8 m. Receivers are mounted on tables at a height of 1.4 m with each patch antenna perpendicular to the ground at a slight angle to capture

the tag's movement. The tag is also perpendicular to the ground and elevated at a height of 0.4 m.

- Cross configuration: Transmitter is located at (5, 9) meter, receivers are located at the points (0, 8), (6.5, 17.5), (12.5, 8.8), (6.3, 0). Transmitter antennae separated by 0.4 m are placed perpendicular to the ground at a height of 1.8 m. Receivers are mounted on tables at a height of 1.4 m with each patch antenna perpendicular to the ground at a slight angle to capture the tag's movement. The tag is also perpendicular to the ground and elevated at a height of 0.4 m.

2) Operational specifications

The dataset utilized in this paper was obtained using the INLAN RFID system. Unlike conventional RFID systems, which are limited to a sub-10-meter reading range, the INLAN system enables ultra-long-range reading capability over 30 meters, positioning RFID technology as a viable solution for real-time localization. This extended range is achieved by introducing harmonic RFID tags in conjunction with a distributed bi-static configuration, in contrast to the conventional mono-static setup used in RFID readers. In this setting, a transmitter operates at the 915 MHz frequency band, illuminating the RFID tag. INLAN harmonic RFID tags receive this 915 MHz signal and respond at 1.83 GHz. The response signal is captured by multiple receivers distributed across the monitoring environment. Each receiver has three heterodyne lines, which measure the signal's strength. In the presented experiments, two of the three lines measure the received power at both x- and y-polarizations. The measured data is then transferred back to the transmitter, which also acts as the system's gateway.

TABLE I: Performance of our MTLoc model compared to four other models: source-only, GRL-based domain adaptation, SFDA, and oracle. Mean Absolute Error (MAE) values were obtained over 5 runs, excluding the source-only approach that was pre-trained on the source dataset and evaluated on the target set.

| Method | Source-free | Dataset | MAE (x) ↓ | MAE (y) ↓ |
|---|-------------|---------|-------------|-------------|
| Source-Only | | Cross | 12.34 | 15.50 |
| | | Square | 12.37 | 16.05 |
| Baseline (Adversarial UDA inspired by freeLoc [42]) | ✗ | Cross | 2.21 ± 0.01 | 7.58 ± 0.02 |
| | ✗ | Square | 2.31 ± 0.01 | 7.63 ± 0.02 |
| MTLoc (Our Model) | ✓ | Cross | 1.81 ± 0.21 | 4.76 ± 0.41 |
| | ✓ | Square | 1.84 ± 0.26 | 4.66 ± 0.46 |
| MTLoc with confidence (Our Model) | ✓ | Cross | 1.83 ± 0.12 | 4.17 ± 0.06 |
| | ✓ | Square | 1.70 ± 0.13 | 4.15 ± 0.05 |
| Oracle (Supervised Fine-Tuning on Target Data) | | Cross | 0.65 ± 0.01 | 0.89 ± 0.02 |
| | | Square | 0.45 ± 0.04 | 0.87 ± 0.04 |

3) Data collection

Data collection is performed using a laptop running INLAN’s proprietary software, connected to the transmitter via an ethernet cable. An RFID tag mounted on a car follows a pre-programmed path (comprising straight lines spaced a meter apart for the experiments), with its movement synchronized using the software to generate ground truth data. As the car moves at a constant speed of approximately 0.28 m/sec, power readings (in dBm) from each receiver (with two polarizations each) are recorded. The time interval between each reading pair of a given receiver is approximately 0.12 seconds. For the square and cross configurations, the transmitter’s output is periodically switched between two antennas, and the maximum reading is recorded, effectively extending the time between consecutive readings to 0.25 seconds.

B. Comparison with Baseline Models

As previously mentioned, we analyzed our indoor localization frameworks developed based on SFDA, called MTLoc, and MTLoc with confidence, with three baseline models: source-only, Adversarial UDA, and Oracle (see Table I). We utilized INLAN’s Ceiling, Cross, and Square datasets, having 12273, 1485, and 1562 samples, respectively. The data was split into training and testing sets with an 80-20 ratio. To ensure robust evaluation, we used 5-fold cross-validation by further dividing the training set into training and validation subsets. Then, the performance of the models was assessed using the held-out test data. To identify the optimal hyperparameters, we examined the error distances corresponding to various validation losses. Through this analysis, we found that for our Cross dataset, the combination of an alpha value of 0.8, a k value of 2, and x and y threshold coefficients of 5 and 4, respectively, yielded the smallest distance error. Similarly, for the Square dataset, x and y threshold coefficients of 4 and 2 resulted in the minimum distance error. The implementation specifics are introduced below, and respective architectures are described in Appendix A.

Localizer: Our source model is trained using a one-dimensional CNN incorporating 9 layers, with INLAN’s Ceiling dataset, employed in our MTLoc and baseline models.

MTLoc: This approach is based on the mean teacher technique using Student and teacher networks, initialized by our localizer, where our Teacher model is updated by applying EMA with an alpha of 0.7.

MTLoc with confidence: Our enhanced approach follows MTLoc’s methodology, using a confidence-based k-NN method (k=2) and an alpha of 0.8 to adjust uncertain pseudo labels to the nearest confident ones.

Adversarial UDA: Our UDA baseline is created using a localizer initialized by our localizer and a discriminator encompassing three layers.

Source-only: In this pre-adaptation baseline, we tested our unlabeled target datasets (INLAN’s Cross and Square sets) using our source localizer.

Oracle: In this approach, we fine-tuned our localizer with labeled target data.

As shown in Table I, the MAE results for both the x and y values of the source-only model are notably high. This outcome can be due to a significant change in the algorithm’s performance between training on the initial dataset and deployment, commonly referred to as a domain or distributional shift in the environment. For the Oracle method, we utilized labeled data to fine-tune our source model, leading to significantly lower error rates and a reduced margin of error. Among these two models with a maximum and minimum margin of error, other approaches fall in between including our GRL-based UDA model in which we have access to the source data. As the x values represent the distances between pathways, analyzing the y values or their distance (d) could provide a more comprehensive evaluation. With our UDA baseline, we achieved a substantial decrease of error regarding both of the x and y values by $\approx 82\%$ and $\approx 51\%$ for our Cross dataset and $\approx 81\%$ and $\approx 52\%$ for our second target set, using domain adaptation. This substantial improvement aids us in discovering SFDA methods. Our MTLoc model provides a significant improvement in terms of MAE performance. Results indicate that access to source data does not improve the performance of our model. As observed, utilizing MTLoc results in our Cross dataset shows an error reduction of approximately 18% and 37% for x and y positional coordinates, compared to the UDA baseline outcomes. Similarly, experiments on the

Square set show similar results. Furthermore, while analyzing our proposed MTLoc with confidence approach, we noticed a minor improvement compared to the original MTLoc model. Our two-dimensional coordinates obtained a decreased error in both target sets, acquiring enhancement in both positional coordinates. Subsequently, both positional coordinates' standard deviation (σ) have shrunk. While the error improvement seems marginal, the confidence-based approach can be regarded as a more robust model with fewer variations considering the significant improvement in the standard deviation.

C. Ablation Studies

In this section, we observe the impact of hyper-parameter values, including the EMA's alpha, k of our k -NN-based correctional model, and the threshold we set for our x and y -predicted pseudo labels. For this experiment, our MTLoc with confidence model is applied on the same datasets, testing k values of 1, 2, and 3, along with alpha values of 0.6, 0.7, 0.75, and 0.8. Additionally, we applied x and y coefficients for thresholds of 3, 4, 5, and 4, 5, and 6, respectively. The validation and test losses were observed using 5-fold cross-validation. With an alpha of 0.8 and a k value of 2 obtaining optimal results on the validation set for both the Cross and Square datasets using threshold coefficients of (5,4) and (4,2), we conducted an ablation study to assess the impact of k and alpha, as shown in Tables II&III. Results indicate that $k = 2$ provides the optimal number of neighbors, minimizing test errors for both x and y in both datasets. The experiment highlights that one neighbor is insufficient for correcting pseudo labels. Increasing k from 1 to 2 or 3 does not significantly affect performance, confirming the reliability of both as hyperparameters. For EMA's alpha, $\alpha = 0.8$ achieves the best performance with more stability. In contrast, a higher α of 0.9 introduces over-smoothing, resulting in notable performance degradation. Additional details of the ablations on hyperparameters, including further experiments on threshold coefficients, are provided in Appendix B.

TABLE II: *Ablation Results on k* : The test MAE values and test distance errors (with standard deviations) are reported for the Cross and Square datasets at $K = 1, 2, 3$, along with $\alpha = 0.8$. For the Cross dataset, the x and y threshold coefficients are set to (5,4), respectively, while for the Square dataset, the thresholds are (4,2).

| k | Dataset | Test MAE (x) ↓ | Test MAE (y) ↓ |
|----------|---------------|--------------------|--------------------|
| 1 | Cross | 1.96 ± 0.21 | 4.28 ± 0.16 |
| | Square | 1.74 ± 0.14 | 4.35 ± 0.24 |
| 2 | Cross | 1.83 ± 0.12 | 4.17 ± 0.06 |
| | Square | 1.70 ± 0.13 | 4.15 ± 0.05 |
| 3 | Cross | 1.88 ± 0.13 | 4.15 ± 0.04 |
| | Square | 1.70 ± 0.09 | 4.19 ± 0.10 |
| 4 | Cross | 1.77 ± 0.12 | 4.73 ± 0.53 |
| | Square | 1.68 ± 0.08 | 4.34 ± 0.15 |

TABLE III: *Ablation Results on α* : The test MAE values and validation distance errors are shown for the Cross and Square datasets at varying α values. The x and y threshold coefficients are set to (5,4) for the Cross and (4,2) for the Square datasets.

| α | Dataset | MAE (x) ↓ | MAE (y) ↓ |
|-------------|---------------|--------------------|--------------------|
| 0.75 | Cross | 1.92 ± 0.23 | 4.44 ± 0.40 |
| | Square | 1.73 ± 0.23 | 4.22 ± 0.16 |
| 0.80 | Cross | 1.83 ± 0.12 | 4.17 ± 0.06 |
| | Square | 1.70 ± 0.13 | 4.15 ± 0.05 |
| 0.85 | Cross | 1.83 ± 0.26 | 4.47 ± 0.25 |
| | Square | 1.89 ± 0.28 | 4.11 ± 0.14 |
| 0.90 | Cross | 3.17 ± 1.28 | 4.89 ± 0.87 |
| | Square | 3.11 ± 0.27 | 5.80 ± 0.49 |

V. CONCLUSIONS

Data privacy, storage, transfer costs, and domain shifts are critical challenges in UDA, often affecting model performance in localization tasks. To address these concerns, an SFDA model was proposed for indoor localization that preserves data privacy and reduces transfer costs. In particular, the new MTLoc model is initialized by a localizer with the architecture of a 1D-CNN. MTLoc utilizes a student-teacher architecture that improves stability through an MT mechanism, where the teacher network generates pseudo labels. An enhanced certainty-based approach called "MTLoc with confidence" selectively uses highly confident pseudo labels during training to improve performance. This technique refines the teacher network's pseudo labels by including the two nearest confident labels. In our experimental validation, the MTLoc with confidence model provides lower localization errors compared to baseline methods, including adversarial UDA and SFDA models. The confidence-based approach notably reduced errors in the y dimension and improved stability in both x and y with small variations, resulting in a more robust and reliable model.

Future works should explore semi-supervised techniques in environments with reference tags and validate them on additional datasets. Including labeled target data and fine-tuning models using reference tag information can significantly improve and optimize the performance.

REFERENCES

- [1] Y. Etiabi and E. M. Amhoud. Federated distillation based indoor localization for iot networks. *IEEE Sensors Journal*, 24(7), 2024.
- [2] H. Liu, H. Xue, L. Zhao, D. Chen, Z. Peng, and G. Zhang. Magloc-ar: Magnetic-based localization for visual-free augmented reality in large-scale indoor environments. *IEEE TVCG*, 29(11), 2023.
- [3] Y. Zhao, J. Xu, J. Wu, J. Hao, and H. Qian. Enhancing camera-based multimodal indoor localization with device-free movement measurement using wifi. *IEEE IoTJ*, 7(2), 2020.
- [4] J. H. Seong and D. H. Seo. Selective unsupervised learning-based wi-fi fingerprint system using autoencoder and gan. *IEEE IoTJ*, 7(3), 2020.
- [5] Z. Liu, X. Wang, Z. Chen, M. Zhao, S. Zhang, and J. Li. 3d-fingerprint augment based on super-resolution for indoor 3d wifi localization. In *WCSP*, 2021.
- [6] X. Weng, K.V. Ling, H. Liu, and K. Cao. Towards end-to-end gps localization with neural pseudorange correction. In *FUSION*, 2024.
- [7] Y. Li, B. Yu, and L. Huang. An indoor uwb localization method based on adaptive channel bias estimation. *IEEE Sensors Journal*, 25(1):1339–1349, 2025.

- [8] Y. Huang, S. Mazuelas, F. Ge, and Y. Shen. Indoor localization system with nlos mitigation based on self-training. *IEEE TMC*, 22(7), 2023.
- [9] Z. Gao, Y. Ma, K. Liu, X. Miao, and Y. Zhao. An indoor multi-tag cooperative localization algorithm based on nmbs for rfid. *IEEE Sensors Journal*, 17(7):2120–2128, 2017.
- [10] L. Yang, Y. Chen, X.-Y. Li, C. Xiao, M. Li, and Y. Liu. Tagoram: Real-time tracking of mobile rfid tags to high precision using cots devices. In *MobiCom*, 2014.
- [11] T. M. T. Dinh, N. S. Duong, and K. Sandrasegaran. Smartphone-based indoor positioning using ble ibeacon and reliable lightweight fingerprint map. *IEEE Sensors Journal*, 20(17):10283–10294, 2020.
- [12] Y. Yu, R. Chen, L. Chen, X. Zheng, D. Wu, W. Li, and Y. Wu. A novel 3-d indoor localization algorithm based on ble and multiple sensors. *IEEE IoTJ*, 8(11), 2021.
- [13] W. Zhu, J. Cao, Y. Xu, L. Yang, and J. Kong. Fault-tolerant rfid reader localization based on passive rfid tags. *IEEE TPDS*, 25(8), 2014.
- [14] C.-S. Cheng, H. H. Chang, Y.-T. Chen, T.-H. Lin, P.-C. Chen, C.-M. Huang, H. S. Yuan, and W. C. Chu. Accurate location tracking based on active rfid for health and safety monitoring. In *ICBBE*, 2009.
- [15] W.-H. Chen, H. H. Chang, T.-H. Lin, P.-C. Chen, L.-K. Chen, S. J. Hwang, D. H. Yen, H. S. Yuan, and W. C. Chu. Dynamic indoor localization based on active rfid for healthcare applications: A shape constraint approach. In *BMEI*, 2009.
- [16] H. Huang, J. Yang, X. Fang, H. Jiang, and L. Xie. Varifi: Variational inference for indoor pedestrian localization and tracking using imu and wifi rss. *IEEE IoTJ*, 10(10), 2023.
- [17] Z. Xu, B. Huang, B. Jia, and G. Mao. Enhancing wifi fingerprinting localization through a co-teaching approach using crowdsourced sequential rss and imu data. *IEEE IoTJ*, 11(2), 2024.
- [18] A. K. Panja, S. Biswas, S. Neogy, and C. Chowdhury. Dimensionality reduction through multiple convolutional channels for rss-based indoor localization. *IEEE Sensors Journal*, 24(22):37482–37491, 2024.
- [19] D.-H. Kim, A. Farhad, and J.-Y. Pyun. Uwb positioning system based on lstm classification with mitigated nlos effects. *IEEE IoTJ*, 10(2), 2023.
- [20] H. Yang, Y. Wang, C. K. Seow, M. Sun, M. Si, and L. Huang. Uwb sensor-based indoor los/nlos localization with support vector machine learning. *IEEE Sensors Journal*, 23(3):2988–3004, 2023.
- [21] X. Rao, Z. Luo, Y. Luo, Y. Yi, G. Lei, and Y. Cao. Mffaloc: Csi-based multifeatures fusion adaptive device-free passive indoor fingerprinting localization. *IEEE IoTJ*, 11(8), 2024.
- [22] X. Liu, R. Wu, H. Zhang, Z. Chen, Y. Liu, and T. Qiu. Graph temporal convolutional network-based wifi indoor localization using fine-grained csi fingerprint. *IEEE Sensors Journal*, 25(5):9019–9033, 2025.
- [23] L. Terças, H. Alves, C. H. M. de Lima, and M. Juntti. Bayesian-based indoor factory positioning using aoa, tdoa, and hybrid measurements. *IEEE IoTJ*, 11(12), 2024.
- [24] C. Huang, Z. Tian, W. He, K. Liu, and Z. Li. Spotlight: A 3-d indoor localization system in wireless sensor networks based on orientation and rssi measurements. *IEEE Sensors Journal*, 23(21):26662–26676, 2023.
- [25] H. Ye, B. Yang, Z. Long, and C. Dai. A method of indoor positioning by signal fitting and pdda algorithm using ble aoa device. *IEEE Sensors Journal*, 22(8):7877–7887, 2022.
- [26] R. Elbakly and M. Youssef. Robust low-overhead rf-based localization for realistic environments. *IEEE TMC*, 21(6), 2022.
- [27] E. Fernando, O. De Silva, G. K. I. Mann, and R. Gosine. Toward developing an indoor localization system for mavs using two or three rf range anchors: An observability based approach. *IEEE Sensors Journal*, 22(6):5173–5187, 2022.
- [28] T. Wang, Y. Li, J. Liu, K. Hu, and Y. Shen. Multipath-assisted single-anchor localization via deep variational learning. *IEEE TWC*, 2024.
- [29] Z. Chen, M. I. AlHajri, M. Wu, N. T. Ali, and R. M. Shubair. A novel real-time deep learning approach for indoor localization based on rf environment identification. *IEEE Sensors Letters*, 4(6):1–4, 2020.
- [30] J. Yan, L. Wan, W. Wei, X. Wu, W. P. Zhu, and D. P. K. Lun. Device-free activity detection and wireless localization based on cnn using channel state information measurement. *IEEE Sensors Journal*, 21(21):24482–24494, 2021.
- [31] Q. Ye. Se-loc: Security-enhanced indoor localization with semi-supervised deep learning. *IEEE TNSE*, 10(5), 2023.
- [32] Y. Ruan, L. Chen, X. Zhou, Z. Liu, X. Liu, G. Guo, and R. Chen. ipos-5g: Indoor positioning via commercial 5g nr csi. *IEEE IoTJ*, 10(10), 2023.
- [33] Y. Li, S. Mazuelas, and Y. Shen. A variational learning approach for concurrent distance estimation and environmental identification. *IEEE TWC*, 22(9), 2023.
- [34] S. L. Ayinla, A. A. Aziz, and M. Drieberg. Salloc: An accurate target localization in wifi-enabled indoor environments via sae-alstm. *IEEE Access*, 12, 2024.
- [35] M. Liu, X. Liao, Z. Gao, and Q. Li. Ft-loc: A fine-grained temporal features-based fusion network for indoor localization. *IEEE IoTJ*, 11(3), 2024.
- [36] Z. Chen, H. Zou, J. Yang, H. Jiang, and L. Xie. Wifi fingerprinting indoor localization using local feature-based deep lstm. *IEEE Systems Journal*, 14(2):3001–3010, 2020.
- [37] S. A. Junoh and J.-Y. Pyun. Augmentation of fingerprints for indoor ble localization using conditional gans. *IEEE Access*, 12, 2024.
- [38] Q. Li, H. Qu, Z. Liu, N. Zhou, W. Sun, S. Sigg, and J. Li. Af-dcgan: Amplitude feature deep convolutional gan for fingerprint construction in indoor localization systems. *IEEE TETCI*, 5(3), 2021.
- [39] W. Wu. A meta-learning approach for device-free indoor localization. *IEEE Communications Letters*, 27(3), 2023.
- [40] X. Chen, H. Li, C. Zhou, X. Liu, D. Wu, and G. Dudek. FiDo: Ubiquitous fine-grained localization for unlabelled users via domain adaptation. Association for Computing Machinery, 2020.
- [41] H. Li, X. Chen, J. Wang, D. Wu, and X. Liu. DAFI: Wifi-based device-free indoor localization via domain adaptation. *PProceedings of the ACM on IMWUT*, 5(4), 2021.
- [42] D. Yan, F. Shang, P. Yang, F. Han, Y. Yan, and X.-Y. Li. freeLoc: Wireless-based cross-domain device-free fingerprints localization to free user’s motions. *IEEE IoTJ*, 2024.
- [43] J. Li, Z. Yu, Z. Du, L. Zhu, and H. T. Shen. A comprehensive survey on source-free domain adaptation. *IEEE TIEEE TPAMI*, 46(8):5743–5762, 2024.
- [44] M. Long, Y. Cao, J. Wang, and M. Jordan. Learning transferable features with deep adaptation networks. In *ICML*, 2015.
- [45] S. Cui, S. Wang, J. Zhuo, L. Li, Q. Huang, and Q. Tian. Towards discriminability and diversity: Batch nuclear-norm maximization under label insufficient situations. In *CVPR*, 2020.
- [46] C. Shui and et al. Towards more general loss and setting in unsupervised domain adaptation. *IEEE TKDE*, 35(10):10140–10150, Oct. 2023.
- [47] M. Long, Z. Cao, J. Wang, and M. I. Jordan. Conditional adversarial domain adaptation. In *Proc. Adv. Neural Inf. Process. Syst.*, 2018.
- [48] E. Tzeng, J. Hoffman, K. Saenko, and T. Darrell. Adversarial discriminative domain adaptation. In *CVPR*, 2017.
- [49] J. Li, M. Jing, H. Su, K. Lu, L. Zhu, and H. T. Shen. Faster domain adaptation networks. *IEEE TKDE*, 34(12):5770–5783, Dec. 2022.
- [50] Q. Lian, F. Lv, L. Duan, and B. Gong. Constructing self-motivated pyramid curriculums for cross-domain semantic segmentation: A non-adversarial approach. In *Proc. IEEE/CVF Int. Conf. Comput. Vis.*, 2019.
- [51] Y. Zou, Z. Yu, B. Kumar, and J. Wang. Unsupervised domain adaptation for semantic segmentation via class-balanced self-training. In *ECCV*, 2018.
- [52] J. Li, Z. Du, L. Zhu, Z. Ding, K. Lu, and H. T. Shen. Divergence-agnostic unsupervised domain adaptation by adversarial attacks. *IEEE TPAMI*, 44(11):8196–8211, Nov. 2022.
- [53] M. Zhang, Z. Fan, R. Shibasaki, and X. Song. Domain adversarial graph convolutional network based on rssi and crowdsensing for indoor localization. *IEEE IoTJ*, 10(15), 2023.
- [54] Z. Xu, B. Huang, B. Jia, and G. Mao. Enhancing wifi fingerprinting localization through a co-teaching approach using crowdsourced sequential rss and imu data. *IEEE IoTJ*, 11(2), 2024.
- [55] L. Zhang, S. Wu, T. Zhang, and Q. Zhang. Automatic radio map adaptation for robust indoor localization with dynamic adversarial learning. *IEEE TII*, 2024.
- [56] G. Prasad, A. Pandey, and S. Kumar. Domain adaptation for localization using combined autoencoder and gradient reversal layer in dynamic iot environment. *IEEE TNSE*, 11(1), 2024.
- [57] L. Zhang, S. Wu, T. Zhang, and Q. Zhang. Robloc: Robust wireless localization with dynamic self-adaptive learning. *IEEE IoTJ*, 11(10), 2024.
- [58] X. Chen, H. Li, C. Zhou, X. Liu, D. Wu, and G. Dudek. Fidora: Robust wifi-based indoor localization via unsupervised domain adaptation. *IEEE IoTJ*, 9(12), 2022.
- [59] Y. Kim, D. Cho, and S. Hong. Towards privacy-preserving domain adaptation. *IEEE SPL*, 27, 2020.
- [60] Y. Fang, P.-T. Yap, W. Lin, H. Zhu, and M. Liu. Source-free unsupervised domain adaptation: A survey. *Neural Networks*, 164, 2024.
- [61] J. Li, Z. Yu, Z. Du, L. Zhu, and H. T. Shen. A comprehensive survey on source-free domain adaptation. *IEEE TIEEE TPAMI*, 46(8), 2024.
- [62] J. Pei, Z. Jiang, A. Men, L. Chen, Y. Liu, and Q. Chen. Uncertainty-induced transferability representation for source-free unsupervised domain adaptation. *IEEE TIP*, 32, 2023.

- [63] Y. Yu, S. Shin, S. Back, M. Ko, S. Noh, and K. Lee. Domain-specific block selection and paired-view pseudo-labeling for online test-time adaptation. In *CVPR*, 2024.
- [64] C. M. Bishop and N. M. Nasrabadi. *Pattern recognition and machine learning*, volume 4. Springer, 2006.
- [65] S. Varailhon, M. Aminbeidokhti, M. Pedersoli, and E. Granger. Source-free domain adaptation for yolo object detection. In *ECCVw*, 2024.
- [66] A. Belal, A. Meethal, F. P. Romero, M. Pedersoli, and E. Granger. Multi-source domain adaptation for object detection with prototype-based mean teacher. In *WACV*, 2024.
- [67] Y. Ganin and V. Lempitsky. Unsupervised domain adaptation by backpropagation. In *Proc. of the 32nd Int. Conf. Mach. Learn.*, 2015.
- [68] T. Huang, Y. Zhang, M. Zheng, S. You, F. Wang, C. Qian, and C. Xu. Knowledge diffusion for distillation. *NeurIPS*, 36, 2024.
- [69] N. Mehregan, B. Bozkurt, E. Granger, M. Hajikhani, and M. Shateri. Inlan-indoor localizationse-loc: Security-enhanced indoor localization with semi-supervised deep learning. *IEEE DataPort*, 20253.

VI. APPENDIX A: MODELS IMPLEMENTATION

In this section, implementation details of the MTLoc, and MTLoc with confidence along with the three baselines, Adversarial UDA, Source-only, and Oracle models are provided. In this study, a localizer, pre-trained on the INLAN’s Ceiling dataset, was designed and used in our source-only, UDA baseline and proposed SFDA approaches. An Adam optimizer with a learning rate of 0.001 was used for the optimization.

Source-only: In our source-only model, we used a localizer, having a feature extractor and a regressor. *Feature Extractor:*

- Conv1D (filters = 64, kernel size = 2, activation = ‘ReLU’)
- Dropout (rate = 0.2)
- Conv1D (filters = 128, kernel size = 2, activation = ‘ReLU’)
- Dropout (rate = 0.2)
- Flatten

Regressor:

- Dense (units = 128, activation = ‘ReLU’)
- Dropout (rate = 0.2)
- Dense (units = 64, activation = ‘ReLU’)
- Dense (units = 2)

Adversarial UDA: In our Adversarial UDA baseline, we used a localizer having a feature extractor and regressor with the same structure as our source-only model, together with a discriminator.

Discriminator:

- Dense (units = 128, activation = ‘ReLU’)
- Dense (units = 64, activation = ‘ReLU’)
- Dense (units = 1, activation = ‘Sigmoid’)

MTloc: In our MTLoc model, the teacher and student networks share the same architecture as the localizer. The teacher receives INLAN’s Cross and Squares datasets, while the student processes their noisy variants (variance = 0.1) as unlabeled target data. Using EMA with $\alpha = 0.7$, the teacher’s parameters gradually align with the student’s. In our confidence-based approach, we refine pseudo-labels by defining a threshold where the predicted (x, y) coordinates are adjusted by adding 5 and 3 times their respective standard deviations. Uncertain labels are then corrected as discussed in Algorithm 3 of The Proposed MTLoc Methods.

Oracle: In the Oracle model, we finetune our localizer, previously presented, on labeled target data (INLAN’s Cross and Square datasets).

VII. APPENDIX B: THRESHOLD ABLATION STUDY

As part of our study on the MTLoc with confidence model, we explored different hyperparameter values across two target datasets to better understand its behavior. Each experiment included validation and test results with standard deviations obtained via 5-fold cross-validation. Specifically, we tested x values of 4, 5, and 6, and y values of 2, 3, and 4, which define the threshold. Using the cross and square datasets, we derived matrices of dimensions 1485×1 and 1562×1 for the x and y coordinates, respectively. In the correction module, each training sample underwent 10 iterations with added random noise, producing matrices of size $1485 \times 10 \times 2$ and $1562 \times 10 \times 2$, where the last dimension represents the x and y coordinates.

TABLE IV: Ablation results on threshold coefficients c_x and c_y for $K = 2$ and $\alpha = 0.8$

| (c_x, c_y) | Dataset | Test MAE (x) | Test MAE (y) |
|---------------|--------------|-----------------------------------|-----------------------------------|
| (4, 2) | Cross | 1.78 ± 0.07 | 4.56 ± 0.48 |
| | Square | 1.70 ± 0.13 | 4.15 ± 0.05 |
| (4, 3) | Cross | 1.78 ± 0.16 | 4.39 ± 0.22 |
| | Square | 1.85 ± 0.25 | 4.27 ± 0.19 |
| (4, 4) | Cross | 2.02 ± 0.23 | 4.16 ± 0.05 |
| | Square | 1.73 ± 0.09 | 4.28 ± 0.11 |
| (5, 2) | Cross | 1.88 ± 0.19 | 4.52 ± 0.31 |
| | Square | 1.64 ± 0.05 | 4.24 ± 0.10 |
| (5, 3) | Cross | 1.97 ± 0.17 | 4.60 ± 0.57 |
| | Square | 1.66 ± 0.10 | 4.72 ± 0.61 |
| (5, 4) | Cross | 1.83 ± 0.12 | 4.17 ± 0.06 |
| | Square | 1.80 ± 0.13 | 4.27 ± 0.15 |
| (6, 2) | Cross | 2.22 ± 0.53 | 4.41 ± 0.21 |
| | Square | 1.71 ± 0.06 | 4.27 ± 0.21 |
| (6, 3) | Cross | 1.96 ± 0.11 | 4.60 ± 0.54 |
| | Square | 1.65 ± 0.04 | 4.13 ± 0.05 |
| (6, 4) | Cross | 1.74 ± 0.05 | 4.46 ± 0.37 |
| | Square | 1.82 ± 0.22 | 4.70 ± 0.57 |

After obtaining the outputs, we computed the standard deviation across the 10 noise-augmented iterations for each sample, yielding σ_x and σ_y . The threshold is defined as $T_{thr} = \mu + c \cdot \sigma$, where μ and σ represent the mean and standard deviation of σ_x or σ_y , respectively, and c (c_x or c_y) is the scaling coefficient. This threshold detects high-uncertainty samples, enabling the correction module to adjust pseudo labels accordingly, thereby enhancing robustness. Table IV presents an ablation study on threshold coefficients with $k = 2$ and $\alpha = 0.8$.